

A Novel Arrangement of Feedback Linearization, Sliding Mode Control, Multi-Objective Optimization and Fuzzy Logic for Nonlinear Under-Actuated Systems

M. J. Mahmoodabadi^{1,*}, S. Verdipour Lomer¹, and M. S. Bahraini²

¹ Department of Mechanical Engineering, Sirjan University of Technology, Sirjan, Iran.

² Intelligent Automation Centre, Wolfson School of Mechanical, Electrical & Manufacturing Engineering, Loughborough University, Loughborough LE11 3TU, UK

*Corresponding author: mahmoodabadi@sirjantech.ac.ir

Manuscript received 18 March, 2024; revised 27 October, 2024; accepted 3 November, 2024. Paper no. JEMT-2403-1498.

In this research, a novel fuzzy optimal robust control approach based on the feedback linearization scheme is introduced for a nonlinear under-actuated ball-wheel system. At first, the feedback linearization idea is employed to transform the nonlinear formulations of the ball-wheel system to the linear terms via changing variables instead of approximating them. Then, a robust sliding mode control technique is directed to stabilize the respected under-actuated system. The optimum values of the parameters associated to the designed controller are obtained via a multi-objective optimization process established on the Non-dominated Sorting Genetic Algorithm II (NSGA II). Eventually, a fuzzy logic-based system is designed to enhance the performance of the control system. Comparison of the simulations obviously indicates that the recommended schemes including the sliding mode control, multi-objective optimization and fuzzy system are valid approaches to improve the stabilization task of the feedback linearization idea for the ball-wheel system.

Keywords: Under-actuated systems, Nonlinear control, Feedback linearization, Fuzzy logic, Multi-objective optimization, Sliding mode.

<http://dx.doi.org/10.22109/jemt.2024.449117.1498>

1. Introduction

Under-actuated mechanisms have attracted the attentions of many researchers in the last decade due to their applications in the real world [1-5]. Besides, many efforts have been made to design various controllers such as feedback linearization methods [6], sliding mode controllers [7], adaptive schemes [8], fuzzy approaches [9], etc. for this type of dynamical systems. In addition, due to the inconsistency between the number of actuators and the system degree-of-freedom on one hand and their applications in different fields of the industry on the other hand, it is aimed to design hybrid control methods to have more appropriate performance for such systems. Among the scientific researches, Ming et al. [10] have designed a controller for a ball-wheel system using a feedback linearization controller to regulate the position of the ball on the wheel and investigated its stability through experimental and simulation results. In addition, to control an under-actuated ball and beam system optimally, tracking the desired path has been done, and the stability has been guaranteed in [11]. Huang et al. [12] have provided a comparative sliding mode process for nonlinear under-actuated systems.

The basic idea of the feedback linearization method is to transform non-linear dynamics of the system to linear ones, and then employing a simple linear technique to control it. This idea has been broadly utilized to handle different dynamical systems. To name but

a few, Khazaei et al. [13] have presented a feedback linearization control approach for converters having filters for the weak grid integration. Martins et al. [14] have offered a feedback linearization methodology stabilization for control of quadrotors having zero dynamics. Mehraza et al. [15] have suggested an input-output feedback linearization control method synthesized by artificial neural network for grid-tied packed E-cell inverters. Errouissi et al. [16] have extended a disturbance-observer-based feedback linearization control idea for stabilization and accurate voltage tracking of a DC-DC boost converter. Li et al. [17] have recommended an objective holographic feedbacks linearization control technique for a boost converter with constant power loads. Moghtader Arbatsofla et al. [18] have advocated a fuzzy fractional-order adaptive robust feedback linearization control optimized by the multi-objective artificial hummingbird algorithm for a nonlinear ball-wheel system.

To improve the functioning of control systems, researchers have used different optimization strategies to determine the effective parameters on the objective functions. Chang et al. [19] have investigated the stabilization of a ball and beam system by means of fuzzy robust controllers and optimized its performance by the ant colony algorithm. Sahnehsaraei et al. [20] have utilized approximate feedback linearization and sliding mode reasoning for the stability of an inverted pendulum mechanism by means of genetic optimization. Liu et al. [21] have studied time delay sliding mode systems combined with PID controllers, and adjusted the control gains using the particle

swarm process [22]. Zheng et al. [23] have applied the combination of fuzzy and sliding mode techniques on complex robots in the manifestation of external disturbances. Lawar et al. [24] have designed a single-input-single-output control system to adjust the level of liquid in a reservoir and determined control coefficients by two optimization methods. Xu et al. [25] have proposed a robust control organization by combination of adaptive and fuzzy means to overcome the control problem of complicated systems. Wang et al. [26] have introduced a robust fault-tolerant control theory to stabilize states and guarantee arriving at the sliding surface at a finite time. Moreover, Ma et al. [27] have employed a fractional adaptive integral hierarchical sliding mode policy to command a spherical robot and obtain better execution when facing different disturbances. Hoang et al. [28] have designed a controller through permutation of the feedback linearization idea and the sliding mode tactic based on a dynamical model to reduce the oscillations of the mechanism operating on an elastic base with perfect tracking of the linkages. Fei et al. [29] have developed a controller based on a backstepping scheme and an adaptive fuzzy sliding mode via adjusting the gains having self-learning aptitude and rejecting the nonlinearity terms appeared in governing equations.

Considering stabilization of under-actuated systems, as well as potentials of feedback linearization, sliding mode, fuzzy logic and evolutionary algorithms in control topics, the current work targets to realize an optimal fuzzy robust controller to handle a ball-wheel system. Another purpose of this study is the Pareto design of the announced control schedule by counting two objective functions, containing the summation of settling time and overshoots of the ball and wheel as well as the absolute value of the control voltage through the NSGAIL.

The rest of the current work is as follows. Section 2 represents the dynamical formulations of the regarded nonlinear under-actuated ball-wheel system. In Section 3, basic concepts of the feedback linearization approach, mathematical formulations of the sliding mode policy, terminologies of the fuzzy systems, as well as definitions of the NSGAIL are presented. The proposed control technique as well as the effect of the fuzzy system on the control performance are investigated in Section 4. Further, the attained results are evaluated and compared with those of other approaches in this section. Finally, Section 5 deduces the presented research and exhibits the future studies related to this investigation.

2. Preliminaries

2.1. Full-state feedback linearization

Consider the following state-space formulations related to an arbitrary nonlinear system:

$$\begin{cases} \dot{x} = f(x) + g(x)u \\ y = h(x) \end{cases} \quad (1)$$

where, $x \in R^n$ signifies the vector of the system states, $u \in R$ denotes the vector of the system inputs, and $y \in R^n$ represents the vector of the system outputs. Nonlinear Eq. (1) can be linearized to employ the linear control methods for stabilizing the system. In the feedback linearization approach, the existing nonlinear terms are removed by utilizing the transformation of variables and consequently, the closed-loop dynamics would be linearized. However, in this approach, two following criteria should be satisfied to implement the linearization process [30,31]:

- 1- The control matrix must be full rank (its rank is the highest possible for a matrix of the same dimension).
- 2- Distribution $\Delta = \text{span} [g(x), ad_f g(x), \dots, ad_f^{n-2} g(x)]$ must be involutive ($ad_f g(x)$ denotes the Lie bracket of f and g).

In this way, the desired transformation is defined as the following equation:

$$T(x) = \begin{bmatrix} h(x) \\ L_f h(x) \\ L_f^2 h(x) \\ \vdots \\ L_f^{r-1} h(x) \end{bmatrix} \quad (2)$$

where $L_f h(x)$ represents the Lie derivative of h along f . By applying transformation $T(x)$, nonlinear Eq. (1) can be converted to the following linear system:

$$\begin{cases} \dot{\zeta}_1 = \zeta_2 \\ \dot{\zeta}_2 = \zeta_3 \\ \vdots \\ \dot{\zeta}_n = v \end{cases} \quad (3)$$

where, v represents the control effort of the system that could be considered as the following state feedback formulation.

$$v = -K_1 \zeta_1 - K_2 \zeta_2 - K_3 \zeta_3 - K_4 \zeta_4 \quad (4)$$

To guarantee the stability of the system through a linear feedback control law described in Eq. (4), the numerical values for the components of gain vector $K = [K_1 \ K_2 \ K_3 \ K_4]$ would be properly ascertained. In this way, this control law would establish the asymptotic stability in the area of $\Omega = \{\alpha_1 \ \dot{\alpha}_1 \ \alpha_2 \ \dot{\alpha}_2\}^T \in R^4 \mid |\alpha_1| < \pi/2\}$. Although large angular positions of the ball would result in saturation of the input voltage of the system, which could increase the instability of the system. In this way, by applying some limitations on the motor torque, the attraction area would be reduced.

2.2. Sliding mode-based controller

Sliding mode control as a persuasive attitude has been broadly implemented to stabilize nonlinear systems in the attendance of external disturbances and modeling uncertainties [26,27]. This method has been created on the opinion that control of first-order systems is considerably simpler than control of n-order systems [28]. A time dependent sliding surface could be expressed as follows [25]:

$$S(e, t) = \left(\frac{d}{dt} + \lambda\right)^{n-1} (e) \quad (5)$$

where, λ is the sliding surface parameter having a positive value, n symbolizes the system order, and e demonstrates the output error formulated as $e = y - y_d$ while y is the system output, and y_d represents the desired input. The control effort constructed upon the sliding mode signal is separated into two components: the equivalent law and the switching term [20]. The former is obtained from the time derivative of surface $S(e, t)$ when it is equal to zero. It ensures that the system states meet zero along with the sliding surface. The latter is intended to limit the system into a region nearby surface $S(e, t)$. Based on the above descriptions, the total control law can be declared like this:

$$u = u_{eq} - K_{sw} \text{sat}\left(\frac{S}{\phi}\right) \quad (6)$$

where u_{eq} is the equivalent control law, K_{sw} illustrates the switching coefficient, ϕ presents the thickness of the boundary layer, and sat denotes a continues function (saturation) which is substituted by the sign operator to reduce the chattering occurrence [29].

$$\text{sat}\left(\frac{S}{\phi}\right) = \begin{cases} -1; & \frac{S}{\phi} < -1 \\ \frac{S}{\phi}; & -1 \leq \frac{S}{\phi} \leq 1 \\ 1; & \frac{S}{\phi} > 1 \end{cases} \quad (7)$$

2.3. Fuzzy logic-based systems

Human knowledge can be integrated into real-world plants by applying the fuzzy logic-based systems. In general, three types of fuzzy systems have been introduced in researches: (1) simple

(unmixed), (2) Takagi-Sugeno, and (3) complex (mixed) [32,33]. In the current research work, the latter is exploited to enhance the execution of the designed scheme. A fuzzy logic-based system contains a set of “if-then” statements that expresses the relationship between inputs and outputs in the form of linguistic variables [32]. By considering a fuzzifier as singleton, an inference engine as product and a defuzzifier as center average, the formulation of the fuzzy system could be mentioned as follows:

$$\lambda(x) = \frac{\sum_{l=1}^m \bar{\lambda}^l (\prod_{i=1}^n \mu_{F_i}^l(x_i))}{\sum_{l=1}^m \prod_{i=1}^n \mu_{F_i}^l(x_i)} \quad (8)$$

where, m indicates the number of the rules, n represents the number of the inputs, $\mu_{F_i}^l(x_i)$ are the input membership functions, and $\bar{\lambda}^l$ denotes the centers of the output membership functions.

2.4. Optimization by the NSGA II

The NSGA as the non-dominate sorting genetic algorithm was initially introduced by Zitzler et al. in 2000 for solving multi-objective optimization problems [34]. After that, an adapted form of the NSGA, namely NSGA-II, was developed to present a novel sorting mechanism in 2003 [35]. In this approach, a randomly generated population is initialized and sorted through non-dominated fronts. Each individual in each front is assigned through two parameters; the first one is the fitness value, and the second one is the crowding distance. In this way, the parents are chosen from the population using Tournament selection based on these parameters. The selected population generates new springs by employing the crossover and mutation operators. The new population is ranked again through the non-domination concept, and only the best members would be preferred as the initial population through the fitness value and the crowding distance on the last front.

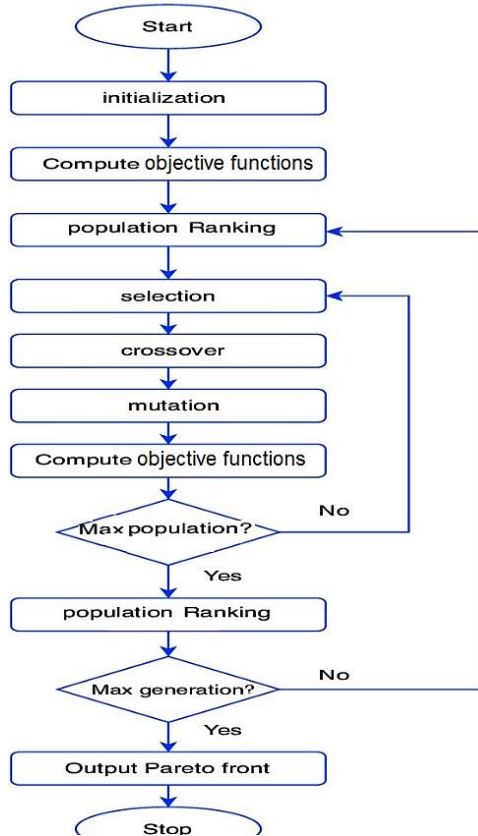


Fig. 1. Flowchart of the NSGA II.

The operation diagram of the NSGA II is exemplified in Fig. 1. In this paper, the first objective function is outlined as the

summation of settling time and overshoot values of the angles of the ball and the wheel, while the absolute value of the control voltage is regarded as the second one.

3. Dynamical modeling of the system

The ball-wheel benchmark system as an under-actuated, unstable, complicated and nonlinear system is studied in this work as schematically shown in Fig. 2. It contains a wheel, a ball and a DC motor as the actuator while the related physical parameters are given in Table 1. The angular location of the ball upon the wheel can be measured by a camera. The controller must adjust the angle of the wheel so that the ball remains in the favorite position upon the wheel. The nonlinear dynamical formulations of the structure would be illustrated as follows [10].

Total kinetic energy K is summation of the kinetic energies of the ball (K_b) and the wheel (K_w) given by

$$K = K_b + K_w = \frac{1}{2}M_b(R_w + R_b)^2\dot{\alpha}_1^2 + \frac{1}{2}J_b\dot{\alpha}_1^2 + \frac{1}{2}J_w\dot{\alpha}_2^2 \quad (9)$$

where J_w denotes the inertia moment for the wheel, R_w represents the wheel radius, M_b illustrates the ball mass, R_b shows the ball radius, and J_b is the inertia moment of the ball given as follow.

$$J_b = \frac{2}{5}M_bR_b^2 \quad (10)$$

Total potential energy P is computed as follows.

$$P = M_bg(R_w + R_b)\cos\alpha_1 \quad (11)$$

where g is the gravitation acceleration.

A familiar form of Euler-Lagrangian formulation could be mentioned as follows.

$$\frac{d}{dt} \left[\frac{\partial EL}{\partial \dot{q}} \right] - \frac{\partial EL}{\partial q} = Q \quad (12)$$

where EL denotes the Euler-Lagrangian function, and q represents the generalized coordinate. Function EL is defined as follows.

$$EL = K + P \quad (13)$$

For this system, two generalized coordinates α_1 and α_2 are regarded (Fig. 3), where α_1 is the angular displacement between y axis and the line through the centers of the ball and the wheel. Finally, α_2 signifies the angular displacement of the wheel. Moreover, the generalized force vector is defined as follows.

$$Q = [0 \quad \tau]^T \quad (14)$$

where torque τ applied on the wheel could be calculated as follows.

$$\tau = \frac{K_m}{R_a}u - \frac{K_m^2}{R_a} \dot{\alpha}_1^2 \quad (15)$$

where R_a denotes the motor resistance, and K_m represents the motor constant. Moreover, u denotes the electrical current of the motor. By considering Eqs. (9) through (15), the formulation of the system dynamics would be written as follows.

$$(7R_b + 7R_w)\ddot{\alpha}_1 - 2R_w\ddot{\alpha}_2 - 5g \sin \alpha_1 \quad (16)$$

$$\left(-\frac{2}{5}R_w^2M_b - \frac{2}{5}R_wR_bM_b\right)\ddot{\alpha}_1 + \left(J_w + \frac{2}{5}R_w^2M_b\right)\ddot{\alpha}_2 = \tau \quad (17)$$

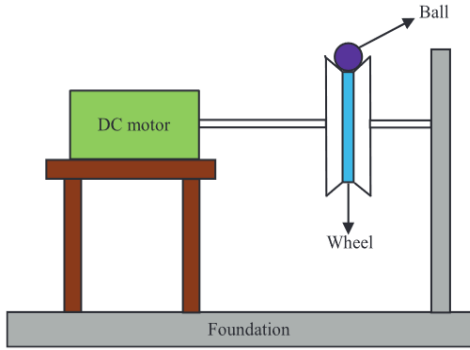
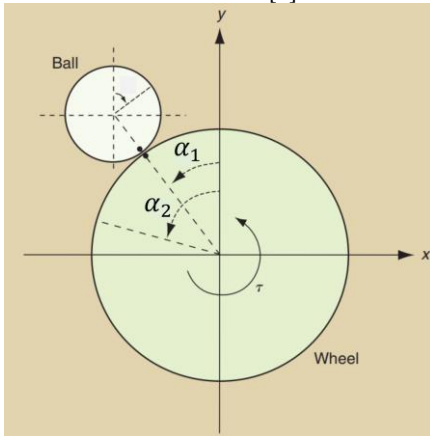
It is supposed that the state vector is considered as $x = [x_1 \quad x_2 \quad x_3 \quad x_4]^T$ that respectively represent α_2 , $\dot{\alpha}_2$, α_1 and $\dot{\alpha}_1$. The formulations of the system in the state-space can be represented as follows.

$$\begin{cases} \dot{x}_1 = x_2 \\ \dot{x}_2 = ax_4 + b \sin x_1 + cu \\ \dot{x}_3 = x_4 \\ \dot{x}_4 = px_4 + q \sin x_1 + ru \end{cases} \quad (18)$$

where, the constant parameters are defined as follows.

Table 1. Parameters of the respected ball-wheel structure.

Value	Symbols	Parameters
Inertia moment for the wheel	J_w	$1.71 \times 10^{-3} \text{ kg} - \text{m}^2$
wheel radius	R_w	0.075 m
Ball mass	M_b	0.042 kg
Ball radius	R_b	0.011 m
Motor resistance	R_a	0.6558Ω
Motor constant	K_m	$0.0662 \text{ N} - \text{m/A}$
Gravitational acceleration	g	9.81 m/s^2

**Fig. 2.** Physical configuration of the ball-wheel system regarded in this research [9]**Fig. 3.** Generalized coordinates of the ball-wheel system studied in this research [10]

$$a = -\frac{2R_w K_m^2}{R_a(7J_w + 2R_w^2 M_b)(R_w + R_b)} \quad (19)$$

$$b = \frac{g(5J_w + 2R_w^2 M_b)}{(7J_w + 2R_w^2 M_b)(R_w + R_b)} \quad (20)$$

$$c = \frac{2R_w K_m}{R_a(7J_w + 2R_w^2 M_b)(R_w + R_b)} \quad (21)$$

$$p = \frac{7K_m^2}{R_a(7J_w + 2R_w^2 M_b)} \quad (22)$$

$$q = \frac{2gR_w M_b}{7J_w + 2R_w^2 M_b} \quad (23)$$

$$r = \frac{7K_m}{R_a(7J_w + 2R_w^2 M_b)} \quad (24)$$

4. Controller design and simulation results

In Fig. 4, a general schematic of the proposed combination of the feedback linearization and fuzzy optimal sliding mode outline is illustrated for the nonlinear under-actuated ball-wheel system. At first step, the dynamical formulations of the ball-wheel system would be linearized using the feedback linearization method represented in Eqs. (3) and (4). By applying the linear transformation on Eq. (2), the following relation for the system

output is obtained.

$$y = h(x) = rx_1 - cx_3 \quad (25)$$

By changing the variables as follows:

$$e_1 = y = rx_1 - cx_3 \quad (26)$$

$$e_2 = L_f h(x) = rx_2 - cx_4 \quad (27)$$

$$e_3 = L_f^2 h(x) = (br - cq) \sin x_1 \quad (28)$$

$$e_4 = L_f^3 h(x) = (br - cq)x_2 \cos x_1 \quad (29)$$

Then, the following control law is formulated [10]:

$$u = \frac{1}{L_g L_f^3 h(x)} [v - L_f^4 h(x)] \quad (30)$$

while, the final linearized formulations could be organized as follows:

$$\dot{e}_1 = e_2 \quad (31)$$

$$\dot{e}_2 = e_3 \quad (32)$$

$$\dot{e}_3 = e_4 \quad (33)$$

$$\dot{e}_4 = v \quad (34)$$

Now, it is possible to design a controller for stabilization of the considered nonlinear under-actuated ball-wheel system. In this fashion, at the start, a linear state feedback controller according to Eq. (35) and based on the pole-placement approach is derived to safeguard the stability of the system.

$$v = -K_1 x_1 - K_2 x_2 - K_3 x_3 - K_4 x_4 \quad (35)$$

where, the numerical values of control gains K_1 , K_2 , K_3 and K_4 are found by employing the pole-placement technique as follows $K = [K_1 \ K_2 \ K_3 \ K_4] = [2019.25 \ 808.5 \ 215.25 \ 6]$. It is noticeable that the initial values for the states of the system are considered as: $[x_1(0) \ x_2(0) \ x_3(0) \ x_4(0)] = [-0.08(\text{rad}) \ 0(\text{rad/s}) \ 0.08(\text{rad}) \ 0(\text{rad/s})]$. In addition, for representation of the system behavior, the phase portraits with various initial conditions are illustrated in Fig. 5. Although the new form of the governing equations is linear, the behavior of this system is inherently nonlinear. Therefore, a robust variable structure sliding mode control idea is designed to conduct the unstable dynamical equations of the considered ball-wheel mechanism.

At first, a time-variable sliding surface is defined according to Eq. (5) for the fourth-order system formulated in Eqs. (31) through (34) as follows.

$$S(e, t) = \left(\frac{d}{dt} + \lambda\right)^3 \tilde{e} = \frac{d^3 \tilde{e}}{dt^3} + 3\lambda \frac{d^2 \tilde{e}}{dt^2} + 3\lambda^2 \frac{d \tilde{e}}{dt} + \lambda^3 \tilde{e} \quad (36)$$

Since the desired input in the ball-wheel system is $y_d = 0$, it can be said that $\tilde{e} = y$.

$$S(y, t) = y^{(3)} + 3\lambda y^{(2)} + 3\lambda^2 y^{(1)} + \lambda^3 y \quad (37)$$

By differentiating the above sliding surface as follows:

$$\begin{aligned} \dot{S}(y, t) = & c(br - cq) \cos x_1 u + \\ & (br - cq) \left((ax_4 + b \sin x_1) \cos x_1 - x_2^2 \sin x_1 \right) + \\ & 3\lambda (br - cq) x_2 \cos x_1 + 3\lambda^2 (br - cq) \sin x_1 + \\ & \lambda^3 (rx_2 - cx_4) \end{aligned} \quad (38)$$

and setting it correspondent to zero, the equivalent control law would be obtained as:

$$\begin{aligned} u_{eq} = & -\frac{1}{c(br - cq) \cos x_1} \left((br - cq) \right. \\ & \left. \left((ax_4 + b \sin x_1) \cos x_1 - x_2^2 \sin x_1 \right) + \right. \\ & \left. 3\lambda (br - cq) x_2 \cos x_1 + 3\lambda^2 (br - cq) \sin x_1 + \right. \\ & \left. \lambda^3 (rx_2 - cx_4) \right) \end{aligned} \quad (39)$$

Eventually, the switching control term is added to smooth the control law according to Eq. (30).

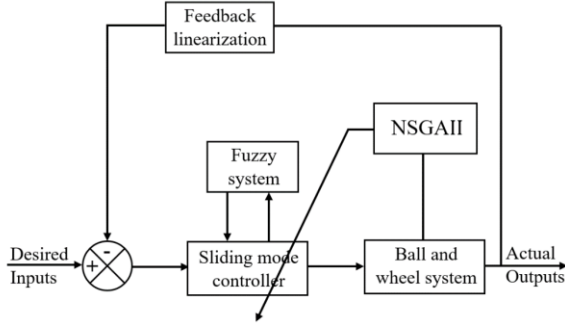


Fig. 4. General schematic of the proposed controller for the nonlinear under-actuated ball-wheel construction.

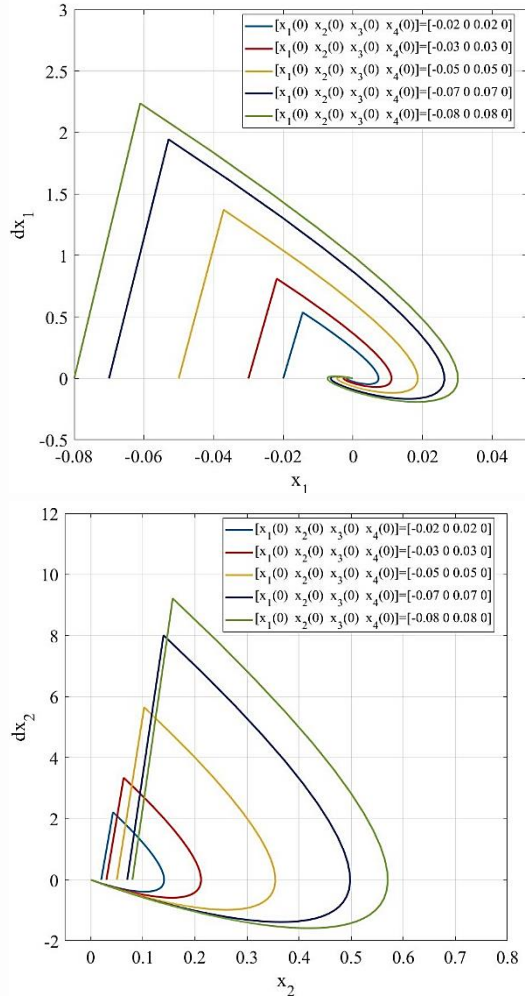


Fig. 5. Phase portraits of the system states for various values of the initial conditions.

After designing the control law, the multi-objective NSGAI is used to enhance its performance. The summation of normalized settling time and the overshoot values of the both ball and wheel are considered as the first objective function, while the integral of the absolute quantity of the control effort is considered as the second one. It is noticeable that these conflicting objective functions should be concurrently minimized to discover the finest values for the sliding mode parameters regarded as design variables $[\lambda \ K_{sw} \ \phi]$. In this regard, the size of the initial population is established at 50, while the termination condition of the optimization progression would be considered as the maximum number of iterations equal to 300.

Table 2. Optimum amounts of the design parameters and the associated objective functions for the selected optimum positions A, B and C shown in Fig. 6.

Optimum position	λ	K_{sw}	ϕ	First objective	Second objective
A	16.397	62.269	68.854	1.607	0.6665
B	10.6926	51.069	68.216	1.879	0.2929
C	23.329	0.583	97.371	2.94	0.0006

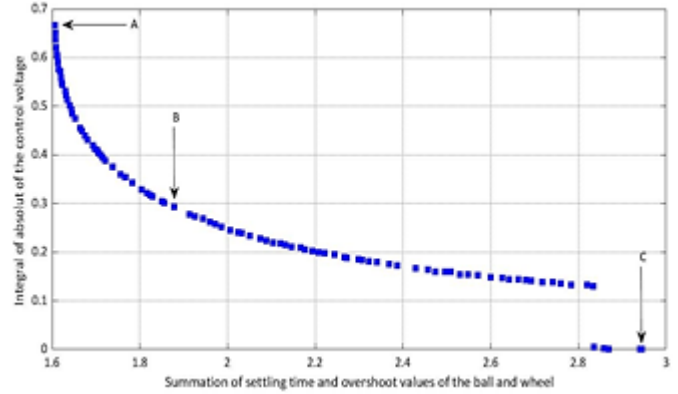


Fig. 6. Pareto front obtained by the multi-objective NSGA II and related to the proposed feedback linearization based sliding mode controller.

In Fig. 6, the Pareto frontage obtained through the multi-criteria optimization process for the sliding mode based on the feedback linearization controller is depicted. All results presented in this figure are non-dominated however, three optimum design points are preferred for investigation and discussion. Point A is the best solution from the perspective of the first objective function, while point C is the best answer from the perspective of the second target. Besides, point B, as a trade-off optimum design solution, satisfies both objective functions, simultaneously. The found optimum design parameters and corresponding goal functions for points A, B and C are enumerated in Table 2. It would be remarked that the obtained control gains for point B would be utilized for comparison and fuzzification of the feedback linearization-based sliding mode control outline.

To enhance the execution of the designed control approach, the numerical value of sliding surface coefficient λ is determined by employing a fuzzy logic-based system. In fact, the simulation results depict that this idea successfully modifies the convergence of the system responses. The considered fuzzy system implements a fuzzifier as the singleton, a defuzzifier as the center average and an inference engine as Mamdani's product formulated as follows:

$$\lambda_{fuzzy} = \frac{\sum_{i=1}^8 P^i N_i(y)}{\sum_{i=1}^8 N_i(y)} \quad (40)$$

where, $N_i (i = 1,2,3, \dots, 8)$ denote the input membership functions as illustrated in Fig. 7, while $P^i (i = 1,2,3, \dots, 8)$ represent the centers of the output membership functions as portrayed in Fig. 8.

As it is apparent from these figures, system error $y = h(x)$ is the input parameter of the fuzzy structure, while sliding surface parameter λ would be its output. In fact, the eight IF-THEN rules could be represented as follows.

$$\text{Rule } i: \text{ IF } y = h(x) \text{ is } N_i \text{ THEN } \lambda \text{ is } P_i \text{ (} i = 1,2, \dots, 8 \text{)} \quad (41)$$

where N_i and P_i are respectively illustrated in Figs. 7 and 8. Fig. 7 shows the distribution of N_i as eight Gaussian membership functions determined through the minimum and maximum values of system error $y = h(x)$ obtained by applying the optimal sliding mode control. Fig. 8 depicts the distribution of P_i as six triangular and two trapezoidal membership functions found via the minimum and maximum quantities of sliding surface parameter λ identified through the

optimization process. In order to investigate the functioning of the introduced control strategies for the regarded nonlinear under-actuated ball-wheel system, the initial amounts of the states are concerned as $[\alpha_1(0) \ \dot{\alpha}_1(0) \ \alpha_2(0) \ \dot{\alpha}_2(0)] = [-0.08 \text{ (rad)} \ 0 \ 0.08 \text{ (rad)} \ 0]$ while the related desired values are fixed at zero. By utilizing the physical configurations listed in Table 1, the time responses of the ball and the wheel are exemplified in Figs. 9 and 10, correspondingly. Further, the designed control efforts as the signal voltages are portrayed in Fig. 11.

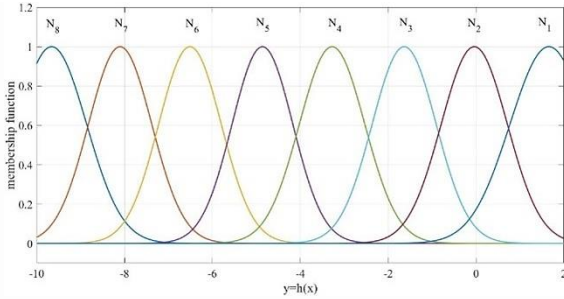


Fig. 7. Input membership functions for the fuzzy structure.

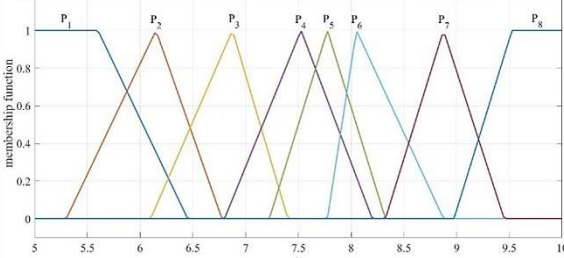


Fig. 8. Output membership functions for the fuzzy structure.

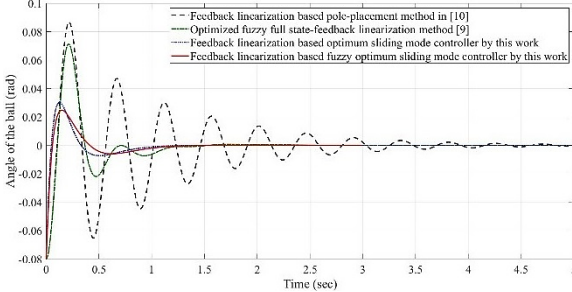


Fig. 9. Time trajectories of the angle of the ball for the different control methods.

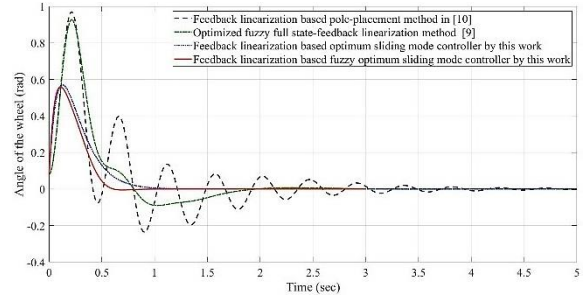


Fig. 10. Time trajectories of the angle of the wheel for the different control methods.

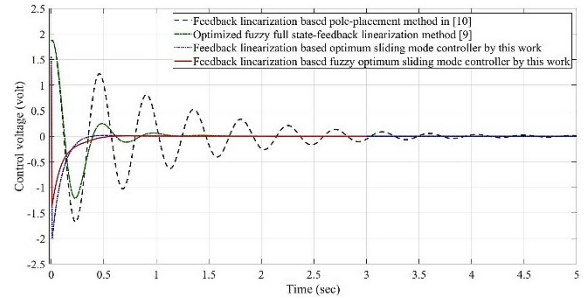


Fig. 11. Time trajectories of the control inputs for the distinct control methods.

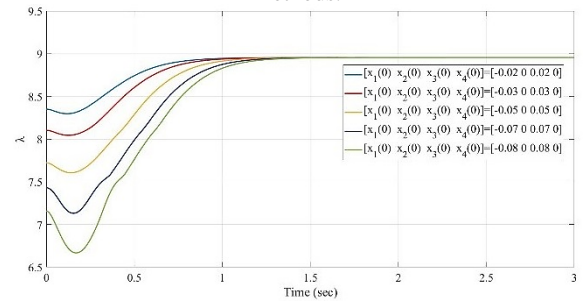


Fig. 12. Sliding surface parameter λ as the output of the fuzzy system for different initial conditions.

Table 3. Settling time and overshoot amounts for the ball and the wheel obtained by applying different control techniques.

Controller	Settling time (sec)		Overshoot (rad)	
	Ball angle	Wheel angle	Ball angle	Wheel angle
Feedback linearization-based pole placement method [10]	4.48	4.17	0.0868	0.971
Optimized fuzzy full state-feedback linearization method [9]	1.25	1.92	0.0691	0.935
Feedback linearization-based optimum sliding mode controller	1.15	1.08	0.0312	0.57
Feedback linearization-based fuzzy optimum sliding mode controller	1.10	0.70	0.0253	0.56

In these illustrations, the performance of the feedback linearization-based fuzzy optimal sliding mode controller is contrasted with those of the other approaches, i.e. the feedback linearization-based optimal sliding mode controller, optimized fuzzy full state-feedback linearization controller [9] and feedback linearization-based pole-placement method [10]. It is clear from these figures that the results of the feedback linearization-based pole-placement approach [10] represent a fluctuating behavior during the stabilization process. Moreover, the optimized fuzzy full state-feedback linearization approach [9] displays a longer settling time and higher overshoot value in comparison with the controllers of this work. Although both other approaches introduced by this work demonstrate more suitable performance to converge the system states to zero, the fuzzy system could significantly improve the overshoot and settling time values. These observations are approved through the numerical values given in Table 3. Moreover, time variations of the fuzzy sliding surface parameter for different values of the initial situations of the states are exposed in Fig. 12.

4. Conclusions and future works

This article exhibited a Pareto optimal pattern of a new fuzzy robust controller employed for stabilization of an under-actuated nonlinear fourth-order system. To this end, the feedback linearization technique removed the nonlinear terms of the governing dynamical equations by changing the variables. Then, a sliding mode controller was invented to handle the system conditions from start situations to final values. Next, a multi-criteria optimization procedure was

implemented to properly indicate the control gains to simultaneously reduce the control effort and output errors. In order to apply the knowledge of experts for tuning the sliding surface parameters, a linguistic IF-THEN rule-based fuzzy system was utilized. Finally, the assessment of results indicated the superiority of the suggested approach for balancing the considered ball-wheel system in appraisal with other feedback linearization-based methods. The following topics could be investigated as the future works of this research study.

- (I) Employing the fractional-order integrals and derivatives to make more flexibility for the designed controller.
- (II) Utilizing adaptive mechanisms for timely tuning the control gains.
- (III) Implementing the proposed fuzzy optimal robust hybrid controller on other nonlinear under-actuator dynamical systems.
- (IV) Applying other multi-objective optimization strategies to discover possible existing Pareto optimum fronts.

References

- [1] D. Rodriguez-Cianca, C. Tom Verstraten, R. Guerrero, R. Jimenez-Fabian, M. B. Naef, B. Vanderborght, and D. Lefeber, "The two-degree-of-freedom cable pulley (2DCP) transmission system: An under-actuated and motion decoupled transmission for robotic applications," *Mechanism and Machine Theory*, vol. 148, 103765, 2020.
- [2] S. Liu, B. Niu, G. Zong, X. Zhao, and N. Xu, "Adaptive fixed-time hierarchical sliding mode control for switched under-actuated systems with dead-zone constraints via event-triggered strategy," *Applied Mathematics and Computation*, vol. 435, 127441, 2022.
- [3] S. Liu, L. Zhang, B. Niu, X. Zhao, and A.M. Ahmad, "Adaptive neural finite-time hierarchical sliding mode control of uncertain under-actuated switched nonlinear systems with backlash-like hysteresis," *Information Sciences*, vol. 599, pp. 147-169, 2022.
- [4] T. Zhao, S. Ding, F. Gao, H. Bian, C. Wang, X. Xu, and K. Hu, "Research on a novel robot mooring system based on dual-parallel elastic under-actuated mechanisms," *Applied Ocean Research*, vol. 119, 103020, 2022.
- [5] N. Xu, Y. Chen, A. Xue, G. Zong, and X. Zhao, "Event-trigger-based adaptive fuzzy hierarchical sliding mode control of uncertain under-actuated switched nonlinear systems," *ISA Transactions*, vol. 124, pp. 301-310, 2022.
- [6] M.J. Mahmoodabadi, and T. Soleymani, "Optimum fuzzy combination of robust decoupled sliding mode and adaptive feedback linearization controllers for uncertain under-actuated nonlinear systems," *Chinese Journal of Physics*, vol. 64, pp. 241-250, 2020.
- [7] A. Mousavi, A.H. Markazi, and E. Khanmirza, "Adaptive fuzzy sliding-mode consensus control of nonlinear under-actuated agents in a near-optimal reinforcement learning framework," *Journal of the Franklin Institute*, vol. 359, pp. 4804-4841, 2022.
- [8] S. Ullah, Q. Khan, A. Mehmood, S.A.M. Kirmani, and O. Mechali, "Neuro-adaptive fast integral terminal sliding mode control design with variable gain robust exact differentiator for under-actuated quadcopter UAV," *ISA Transactions*, vol. 120, pp. 293-304, 2022.
- [9] R. Abedzadeh Maafi, S. Etemadi Haghighi, and M. J. Mahmoodabadi, "A novel multi-objective optimization algorithm for Pareto design of a fuzzy full state feedback linearization controller applied on a ball and wheel system," *Transactions of the Institute of Measurement and Control*, vol. 44, pp. 1388-1409, 2022.
- [10] M.T. Ho, Y.W. Tu, and H.S. Lin, "Controlling a ball and wheel system using full-state-feedback linearization: a testbed for nonlinear control design," *Control Systems Magazine*, 29 (5): pp. 93-101, 2009.
- [11] S. Cardona, S. Ospina, and E. Giraldo, "Sliding mode control based on feedback linearization for a ball and beam system," *4th IEEE Colombian Conference on Automatic Control as Key Support Ind. Product*, pp. 1-5, 2019.
- [12] Y.J. Huang, T.C. Kuo, and S.H. Chang, "Adaptive sliding-mode control for nonlinear systems with uncertain parameters," *IEEE Transactions on Systems, Man, and Cybernetics, Part B (Cybernetics)*, vol. 38, pp. 534-539, 2008.
- [13] J. Khazaei, Z. Tu, A. Asrari, and W. Liu, "Feedback linearization control of converters with LCL filter for weak AC grid integration," *IEEE Transactions on Power Systems*, vol. 36, pp. 3740-3750, 2021.
- [14] L. Martins, C. Cardeira, and P. Oliveira, "Feedback linearization with zero dynamics stabilization for quadrotor control," *Journal of Intelligent & Robotic Systems*, vol. 101, pp. 1-17, 2021.
- [15] M. Mehrasa, M. Babaie, M. Sharifzadeh, and K. Al-Haddad, "An input-output feedback linearization control method synthesized by artificial neural network for grid-tied packed E-cell inverter," *IEEE Transactions on Industry Applications*, vol. 57, pp. 3131-3142, 2021.
- [16] R. Errouissi, H. Shareef, A. Viswambharan, and A. Wahyudie, "Disturbance-observer-based feedback linearization control for stabilization and accurate voltage tracking of a DC-DC boost converter," *IEEE Transactions on Industry Applications*, vol. 58, pp. 6687-6700, 2022.
- [17] J. Li, H. Pan, X. Long, and B. Liu, "Objective holographic feedbacks linearization control for boost converter with constant power load," *International Journal of Electrical Power & Energy Systems*, vol. 134, 107310, 2022.
- [18] S.M. Arbatsofla, A.H. Mazinan, M.J. Mahmoodabadi, and M.A. Nekoui, "Fuzzy fractional-order adaptive robust feedback linearization control optimized by the multi-objective artificial hummingbird algorithm for a nonlinear ball-wheel system," *Journal of the Brazilian Society of Mechanical Sciences and Engineering*, vol. 45, 575, 2023.
- [19] Y.H. Chang, C.W. Chang, C.W. Tao, H.W. Lin, and J.S. Taur, "Fuzzy sliding-mode control for ball and beam system with fuzzy ant colony optimization," *Expert Systems with Applications*, vol. 39, pp. 3624-3633, 2012.
- [20] M.A. Sahnehsaraei, M.J. Mahmoodabadi, and A. Bagheri, "Pareto optimum control of a 2-DOF inverted pendulum using approximate feedback linearization and sliding mode control," *Transactions of the Institute of Measurement and Control*, vol. 36, pp. 496-505, 2014.
- [21] J. Liu, H. An, Y. Gao, C. Wang, and L. Wu, "Adaptive control of hypersonic flight vehicles with limited angle-of-attack," *IEEE/ASME Transactions on Mechatronics*, vol. 23, pp. 883-894, 2018.
- [22] C.C. Soon, R. Ghazali, H.I. Jaafar, and S.Y.S. Hussien, "Sliding mode controller design with optimized PID sliding surface using particle swarm algorithm," *Procedia Computer Science*, vol. 105, pp. 235-239, 2017.
- [23] K. Zheng, Y. Hu, and B. Wu, "Intelligent fuzzy sliding mode control for complex robot system with disturbances," *European Journal of Control*, vol. 51, pp. 95-109, 2020.
- [24] A.R. Laware, D.B. Talange, and V.S. Bandal, "Evolutionary optimization of sliding mode controller for level control system," *ISA Transactions*, vol. 51, pp. 95-109, 2018.
- [25] N. Xu, Y. Chen, A.K. Xue, G.D. Zong, and X.D. Zhao, "Event-trigger-based adaptive fuzzy hierarchical sliding mode control of uncertain under-actuated switched nonlinear systems," *ISA*

- Transactions*, vol. 124, pp. 301-310, 2019.
- [26] J. Wang, F. Fang, X. Yi, and Y. Liu, "Dynamic event-triggered fault estimation and sliding mode fault-tolerant control for networked control systems with sensor faults," *Applied Mathematics and Computation*, vol. 355, pp. 5475-5502, 2021.
- [27] L. Ma, H. Sun, and J. Song, "Fractional-order adaptive integral hierarchical sliding mode control method for high-speed linear motion of spherical robot," *IEEE Access*, vol. 8, pp. 66243-66256, 2020.
- [28] Q. Hoang, J. Park, and S. Lee, "Combined feedback linearization and sliding mode control for vibration suppression of a robotic excavator on an elastic foundation," *Journal of Vibration and Control*, vol. 27, pp. 251-263, 2020.
- [29] J. Fei, Y. Fang, and Zh. Yuan, "Adaptive fuzzy sliding mode control for a micro gyroscope with backstepping controller," *Micromachines*, vol. 11, 968, 2020.
- [30] J. Slotine, and W. Li, "Applied nonlinear control," Englewood Cliffs, Prentice Hall, USA, vol. 199, 705, 1991.
- [31] H. K. Khalil, *Nonlinear systems*, 3rd ed., Upper Saddle River, Prentice Hall, USA, vol. 5, 2002.
- [32] M.J. Mahmoodabadi, and N. Nejadkourki, "Trajectory tracking of a flexible robot manipulator by a new optimized fuzzy adaptive sliding mode-based feedback linearization controller," *Journal of Robotics*, vol. 2, pp. 1-12, 2020.
- [33] N. Wang, and M.J. Er, "Direct adaptive fuzzy tracking control of marine vehicles with fully unknown parametric dynamics and uncertainties," *IEEE Transactions on Control Systems Technology*, vol. 24, pp. 1845-1852, 2016.
- [34] E. Zitzler, K. Deb, and L. Thiele, "Comparison of multiobjective evolutionary algorithms: Empirical results," *Evolutionary Computation*, vol. 8, pp. 173-195, 2000.
- [35] K. Deb, S. Agrawal, A. Pratap, and T. Meyarivan, "A Fast Elitist Non-dominated Sorting Genetic Algorithm for Multi-objective Optimization: NSGA-II." *Parallel Problem Solving from Nature PPSN VI. Lecture Notes in Computer Science*, vol. 1917, 2000.